Elastic parameters prediction under dynamic loading based on the unit cell of composites considering end constraint effect

Wang Meng[1,2], Fei Qingguo[1,2], Zhang Peiwei[1,2]
(1. Institute of Aerospace Machinery Dynamics, Southeast University, Nanjing 211189, China;
2. Department of Engineering Mechanics, Southeast University, Nanjing 210096, China)

Abstract: With the unit cell model of composites and the elastic parameters of constitutes dependent on strain rates, elastic parameters under dynamic loading in fiber direction can be predicted using the explicit dynamic method. Then, off-axial elastic parameters can be obtained with coordinate transformation matrix and end constraint effect. These parameters agree well with experiment results, which proves the accuracy of the method to predict the dynamic parameters of composites. At last, influences of fiber arrangement and fiber volume fraction on predicted results are revealed.
Key words: unit cell model; high strain rate; elastic parameters; explicit dynamic method; end constraint effect

1 Introduction

Composite laminates now are widely used in the aerospace, automobile, civil engineering and so on, which would have the structures subjected to high speed dynamic loading. For the polymer composites, it is well known that the elastic properties of the composite increase with the strain rates, but the failure strain decreases[1]. The elastic properties prediction of polymer composite under high strain rates contributes to the mechanical behavior description of composite structures under dynamic loading.

Composite materials are heterogeneous, the properties of which are determined by the microstructure and the properties of constituents. With the numerical methods and the microstructure of composites, macroscale properties of composites can be obtained and the experimental expenses can be saved. For long fiber reinforced polymer composites, the microstructure is periodic and the representative volume element (RVE) can be derived. With periodic boundary conditions and homogenization theory, the macroscale properties would be predicted[2]. With the structure of woven composites, the stiffness average method and energy method are used to predict elastic parameters of the composites[3]. With the generalized method of cell for the composite microstructure description, the effects of characteristic parameters of the fiber on the elastic properties prediction are revealed[4]. There is few studies about the elastic properties prediction based on the unit cell of composites under high speed loading rates. The viscoelastic prediction was widely used for the concrete[5].

It aims to predict elastic parameters of composite lamina under high speed loading in this study. Basic theories of composites, including the unit cell model, periodic boundary conditions under dynamic loading, dynamic explicit method and end constraint effect, are introduced firstly. Then the elastic parameters of composites, IM7/977-2, are predicted and compared with the experimental results. At last, the effects of fiber distribution and fiber volume fraction on the elastic parameters prediction are analyzed.

2 Finite element model construction

To predict the elastic parameters under high strain rates, the unit cell model of composite lamina is established firstly. Then the rate-dependent constitutive model of the polymer is considered. The periodic boundary conditions in the dynamic explicit method is introduced. With the homogenization theory and the transformation matrix considering the end constraint effect, the elastic in any material direction can be obtained.

2.1 Unit cell model

The composites can be classified as composite lamina, composite laminates, woven composites, stitched composite and so on according to the geometric models of unit cell. As the composite lamina is analyzed in this study, fiber square, diamond, hexagon and random distribution patterns are adopted[4]. The unit cell models in Ref.[6] are used for the analysis.

The polymer matrix is considered to be rate-dependent. The mechanical behavior of the polymer matrix is described with model for considering rate-dependency of metal material in Yen[7,8]. The elastic model for the matrix material is shown in Eq.1.

$$E = E_0\left(1 + C\ln\frac{\dot{\bar{\varepsilon}}}{\dot{\bar{\varepsilon}}_0}\right) \tag{1}$$

where C is a material constant, E is the effective elastic modulus at the effective strain rate $\dot{\bar{\varepsilon}}$, E_0 is the reference elastic modulus at the strain rate $\dot{\bar{\varepsilon}}_0$, $\dot{\bar{\varepsilon}}_0 = 1$ in this study. The effective strain rate is in Eq.2.

$$\dot{\bar{\varepsilon}} = \sqrt{\frac{2}{3}\left[\left(\dot{\varepsilon}_{11} - \dot{\varepsilon}_m\right)^2 + \left(\dot{\varepsilon}_{22} - \dot{\varepsilon}_m\right)^2 + \left(\dot{\varepsilon}_{33} - \dot{\varepsilon}_m\right)^2 + 2\dot{\varepsilon}_{12}^2 + 2\dot{\varepsilon}_{23}^2 + 2\dot{\varepsilon}_{13}^2\right]} \tag{2}$$

where $\dot{\varepsilon}_m = \frac{1}{2}\left(\dot{\varepsilon}_{11} + \dot{\varepsilon}_{22} + \dot{\varepsilon}_{33}\right)$.

Glass fiber would be rate-dependent, however the carbon fiber in this study is rate-independent[1], so the constitutive model for the fiber is linear-elastic in this study.

2.2 Boundary conditions and dynamic explicit method

To accurately predict the macroscale response of the composites, proper boundary conditions should be applied to ensure the displacement and force continuity between the unit cell models. Homogeneous boundary conditions(HBC) and periodic boundary conditions(PBC) are widely used. Under the tensile and compressive loading, the difference between the results predicted from the two boundary conditions is little. However the periodic boundary conditions give the more reasonable shear deformation than the HBC method[9,10]. For more details of PBC application, refer to [10].

Dynamic explicit method is used for the dynamic analysis. Basic theory is the Newton's second law:

$$\ddot{u}_{(t)} = M^{-1}\left(P_{(t)} - I_{(t)}\right) \tag{3}$$

where M is mass matrix, P is the vector of external loading and I is the vector for internal force. Central difference method is used for the response prediction, so compared with the implicit method,

it is conditionally stable. The stable time increment of dynamic explicit analysis depends on minimum element size, material density and modulus due to conditional convergence of finite difference method. As the small element size in micro model will increase computing time by decreasing stable time increment, mass scale method is employed to save simulating time and obtain precise simulation results with increasing stable time increment.

2.3 Lamination theory and end constraint effect

To predict the off-axis elastic parameters, the transformation matrix should be needed. The transformation is in Eq.4

$$T = \begin{bmatrix} m^2 & n^2 & 2mn \\ n^2 & m^2 & -2mn \\ -mn & mn & m^2 - n^2 \end{bmatrix} \tag{4}$$

where $m = \cos\theta$, $n = \sin\theta$.

Due to the anisotropy of the composites, the specimen would have shear deformation without end constraint effect under tensile loading. With the end constraint effect, additional shear stress would appear. So the end constraint effect would have a great influence on the elastic parameters prediction[11,12]. Under the off-axis loading condition, shear stress would appear in the specimen, so the stress-strain relation under the plane condition loaded in the x direction is shown in Eq.5.

$$\begin{Bmatrix} \varepsilon_{xx} \\ \varepsilon_{yy} \\ \gamma_{xy} \end{Bmatrix} = \begin{bmatrix} \bar{S}_{11} & \bar{S}_{12} & \bar{S}_{16} \\ \bar{S}_{12} & \bar{S}_{22} & \bar{S}_{26} \\ \bar{S}_{16} & \bar{S}_{26} & \bar{S}_{66} \end{bmatrix} \begin{Bmatrix} \sigma_{xx} \\ 0 \\ \tau_{xy} \end{Bmatrix} \tag{5}$$

The relation between the realistic measurement results for the elastic parameters labeled with * and results predicted from the unit cell method is shown Eq.6.

$$E_{xx}^{*} = E_{xx} \frac{1 - 2/3\eta}{1 - \eta} \tag{6}$$

where $\eta = \dfrac{6\bar{S}_{16}^2}{\bar{S}_{11}\left(6\bar{S}_{66} + \bar{S}_{11} l^2 / h^2\right)}$, l and h are the length and width of the specimen. E_{xx} is the elastic modulus predicted with the transformation matrix in the x direction.

With the same method, the shear modulus and passion radio is shown in Eq.7 and Eq.8.

$$\frac{1}{G_{12}^{*}} = \left[\frac{1}{E_{xx}^{*}} - \frac{\cos^4\theta}{E_{11}} - \frac{\sin^4\theta}{E_{22}}\right] \Big/ \cos^2\theta \sin^2\theta + \frac{2\nu_{12}}{E_{11}} \tag{7}$$

$$\frac{\nu_{xy}}{\nu_{xy}^{*}} = \frac{1 + \left(\dfrac{\bar{S}_{16}}{\bar{S}_{11}}\right)\beta}{1 + \left(\dfrac{\bar{S}_{16}}{\bar{S}_{12}}\right)\beta} \tag{8}$$

where $\beta = -\dfrac{6\left(\dfrac{h}{l}\right)^2 \left(\dfrac{\bar{S}_{16}}{\bar{S}_{11}}\right)}{1 + 6\left(\dfrac{h}{l}\right)^2 \left(\dfrac{\bar{S}_{66}}{\bar{S}_{11}}\right)}$

3 Model verification

The material system in this study is IM7/977-2. The properties of the constituents are derived from Ref.[13]. Results from Ref.[14] are used to verify the results predicted from the numerical models.

The properties of the material constituents are shown in table.1:

Table 1. Properties of the material constituents

IM7									
$\rho(kg/m^3)$	E_{11} （GPa）	E_{22} （GPa）	E_{33} （GPa）	v_{12}	v_{13}	v_{23}	G_{12} （GPa）	G_{13} （GPa）	G_{23} （GPa）
1780	276	13.8	13.8	0.25	0.25	0.25	20	20	5.52
977-2									
$\rho(kg/m^3)$	$\dot{\varepsilon}_0(1/\sec)$	E_2 （GPa）	v	C					
1310	1	3.52	0.4	0.166					

The geometric and finite element model used to verify the model established is shown in Fig.1 and 2.

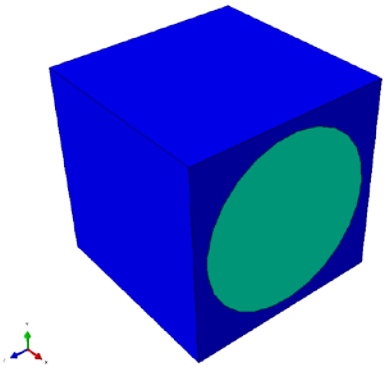

Fig.1 Geometric model for unit cell

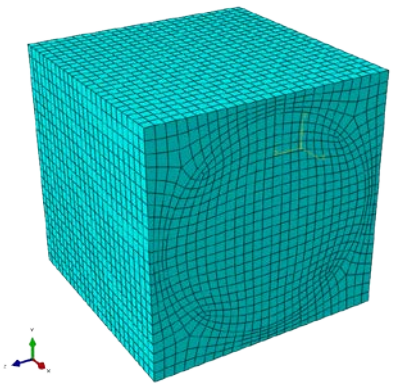

Fig.2 Finite element model for unit cell

In the qusi-static loading condition, loading rates is slow, which contributes to a lot of computation time consumption, so the static-implicit method is adopted for the response analysis. When the model is subjected to dynamic loading with strain rates equaling 400 s^{-1}, the unit cell set here is a cube with length equaling 10mm and the velocity applied at the boundary is 4000mm/s. this scale up of the model size contributes to a easer application of the periodic boundary conditions, as with python method, the point corresponding to the opposite surface should be chosen. The problem of stress oscillation in the unit cell is also raised up. The stress-strain relation in the plane condition is studies and the effects of end constraint on Possion's radio and shear modulus are revealed.

Under high strain rates, effects of density on the stress-strain curves predicted are shown in Fig.3. With the decrease of the material density, stress oscillation in the unit cell would be relieved. The original density parameters for the fiber and matrix are $\rho_f = 1.78\times10^{-9} t/mm^3$ and $\rho_m = 1.31\times10^{-9} t/mm^3$ respectively.

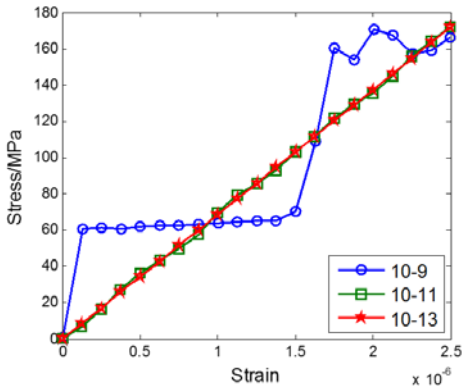

Fig.3 stress-strain curves predicted from the unit cell

According to Ref.[15], the formulations and implementation of PBCs have an impact on results predicted by an explicit solver. A simple fiber square model with node-to-node coupling and absolute formation boundary condition is analyzed by the implicit and explicit solver respectively and the material behaviors are assumed to be elastic. The force-displacement curves are shown in Fig.4. There is little difference between the results obtained, so the formulations and implementation are adopted in the following analysis.

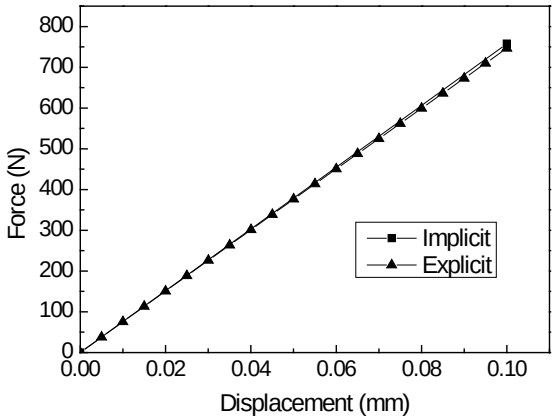

Fig.4 Force-displacement curves obtained with implicit and explicit solver

The length of specimen size in the experiments is 7.9mm and width of it is 2.8mm.The elastic modulus predicted under the qusi-static and dynamic loading in the x direction is shown in Fig.5 and 6.

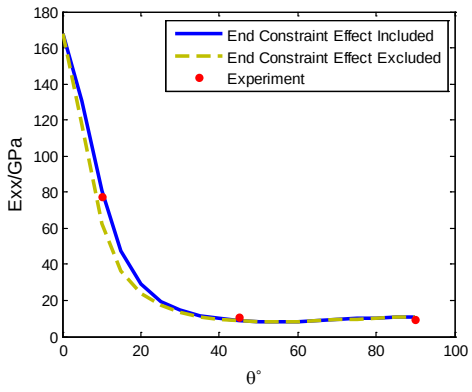

Fig.5 elastic parameters predicted (qusi-static)

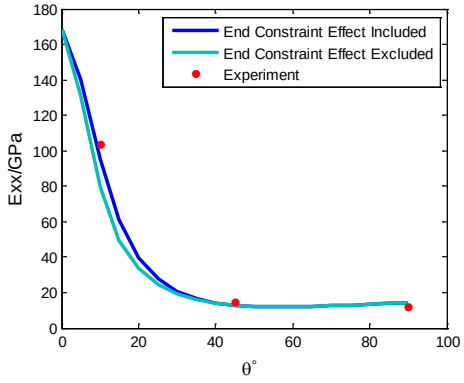

Fig.6 elastic parameters predicted (dynamic)

It can be concluded that the results predicted from models considering the end constraint effect are more consistent with the experimental results, especially for the modulus from the specimen with off-axis angle equaling 10°, which verifies the analytical method used in this study. During the tensile loading, the end constraint will have an impact on the modulus of the results under the static and dynamic condition.

Comparing Fig.5 with 6, the difference between modulus predicted from the qusi-static model and dynamic model is 0.5% in the *x* direction, however, the difference between them in the *y* direction is 22.6%. This results from the reason that the modulus in the *y* direction is more sensitive to the properties of matrix which is strain rate dependent.

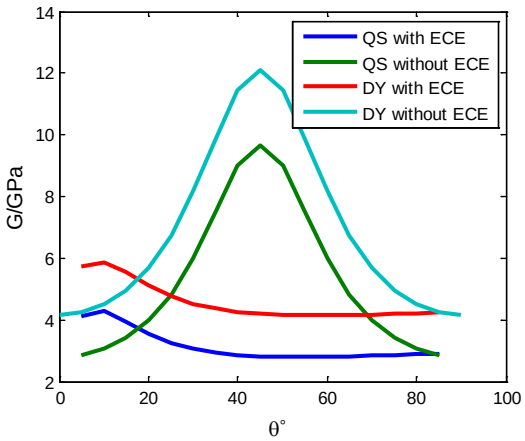

Fig.7 Shear modulus to off-axis angle curves

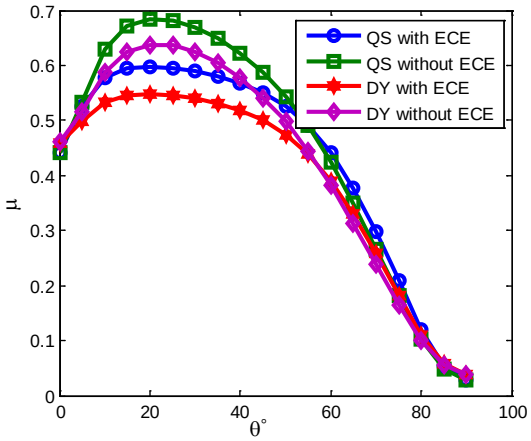

Fig. 8 Possion's radio to off-axis angle curves

The shear modulus to off-axis angle curves are shown in Fig.7. The end constraint effect and loading speed have a great influence on the shear modulus in the specimen. With the increase of the loading speed, the shear modulus increase sharply. The end constraint effect increases the modulus results with low off-axis angle. However, the end constraint effect decreases the modulus results with high off-axis angle

The Possion's radio to off-axis angle curves is shown in Fig.8. The loading speed and end constraint effect have an impact on the results with low off-axis angle. The end constraint effect decreases shear and tensile modulus prediction results, especially for the models with low off-axis angle.

4 Effects of fiber features analysis

The effects of fiber features including fiber distribution and volume fraction on the dynamic elastic parameters predicted are revealed in this section. For simplification, the effect of end constraint is not included. Firstly, the unit cell models with fiber diamond and hexagon distribution patterns are established and analyzed. Then elastic parameters prediction of unit cell models with different fiber volume fraction are conducted.

4.1 Fiber distribution patterns

The models with fiber diamond and hexagon distribution patterns are shown in Fig.9 and 10.

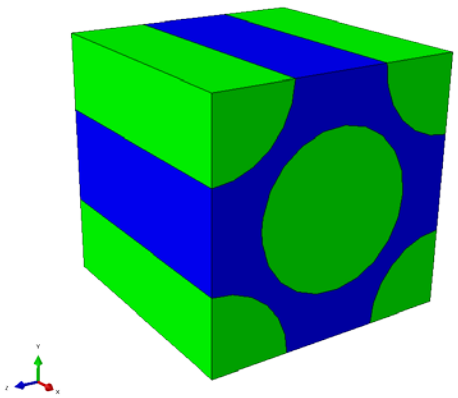

Fig.9 Geometric model with fiber diamond distribution

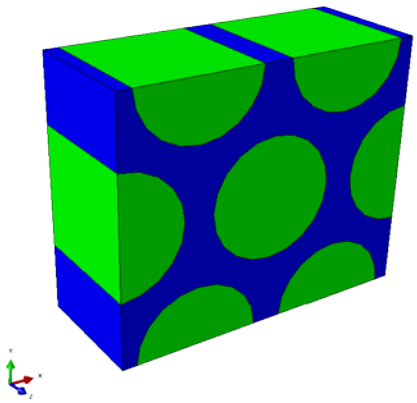

Fig.10 Geometric model with fiber hexagon distribution

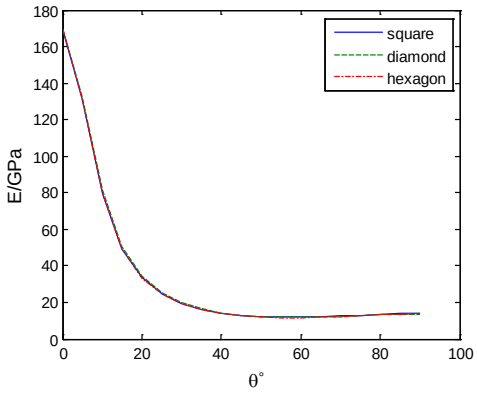

Fig.11 Tensile modulus to off-axis angle curves

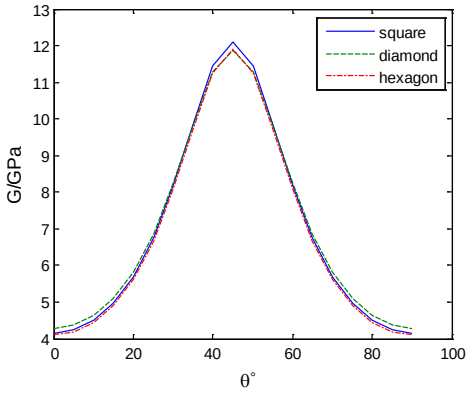

Fig.12 Shear modulus to off-axis angle curves

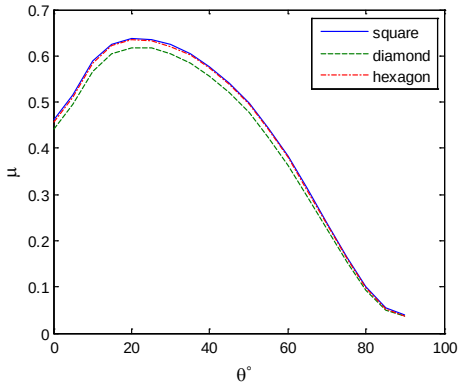

Fig.13 Possion's radio to off-axis angle curves

The results predicted from the models are shown in Fig 11-13. From Fig.11, it can be found that there is little difference for the tensile modulus predicted. However, the shear modulus and Possion's radio predicted from the fiber diamond distribution model is different from those from models with fiber square and hexagon distribution patterns in Fig.12 and 13.

4.2 Fiber volume fraction

The geometric models with different fiber volume fraction (FVF), 20%，40% and 78%, are established in Fig.14, 15 and 16.

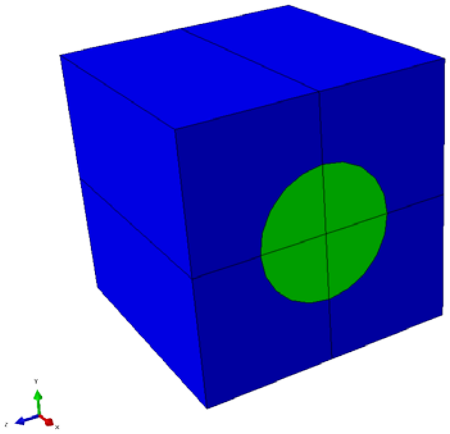

Fig.14 Geometric model with FVF 20%

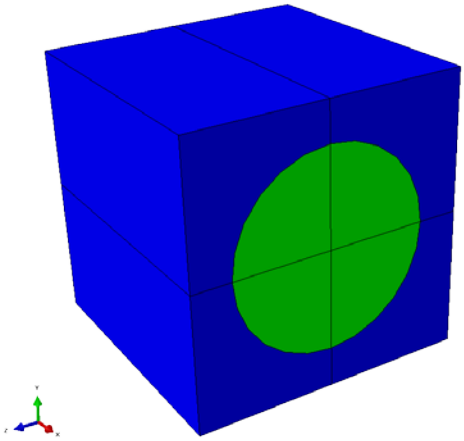

Fig.15 Geometric model with FVF 40%

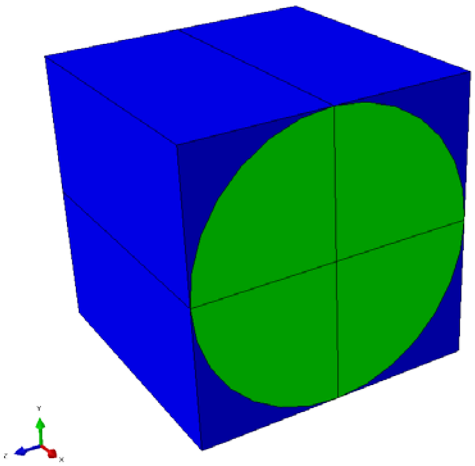

Fig.16 Geometric model with FVF 78%

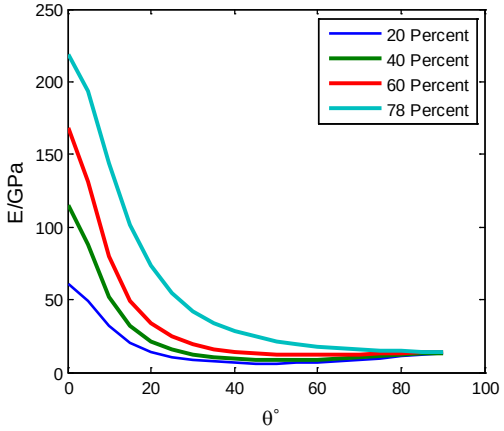

Fig.17 Tensile modulus to off-axis angle curves

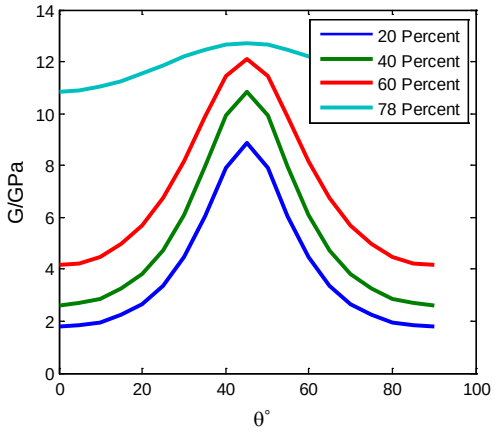

Fig.18 Shear modulus to off-axis angle curves

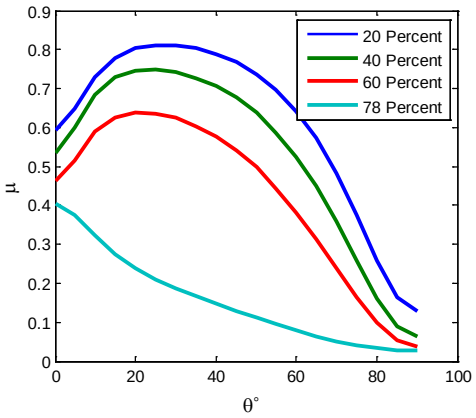

Fig.19 Possion's radio to off-axis angle curves

From the results shown in Fig.17-19, it can be found that the tensile and shear modulus increase with the increase of the fiber volume fraction. However, the Possion's radio decreases.

5 Conclusion

The elastic properties of polymer composites are strain-rate dependent and this study focuses on the properties prediction under dynamic loading. The unit cell models considering the rate-dependency of constituents and periodic microstructure are established for the properties prediction.

The dynamic explicit method and periodic boundary conditions are adopted to analyze the dynamic response of the unit cell. With the homogenization theory, average response of the composite can be obtained and the elastic properties of the polymer composites can be predicted. As the characteristic length of the unit cell is at the submicron degree, it would be difficult for the periodic boundary conditions application and contribute to small time increment for the dynamic explicit method. Proper scale up of the unit cell model is used to increase the time increment and decreasing the densities of the constituents contributes to relieving the concomitant stress oscillation.

With the transformation matrix and end constraint effect, the in-plane elastic properties of polymer composites are predicted and compared with the results without considering the end constraint effect and experimental results. It can be found that the results considering end constraint effect are more close to the experiment results. Then the effects of fiber distribution patterns and fiber volume fraction are revealed with the analytical methods. The results predicted from model with fiber diamond distribution have a little difference from those derived with fiber square and hexagon models. The tensile and shear modulus results predicted increase with the increase of the fiber volume fraction. However, the Possion's radio decreases.

Reference

[1] Park I K, Park K J, Kim S J. Rate-dependent damage model for polymeric composites under in-plane shear dynamic loading[J]. Computational Materials Science, 2015, 96:506-519.

[2] Lu Z, Zhou Y, Yang Z, et al. Multi-scale finite element analysis of 2.5D woven fabric composites under on-axis and off-axis tension[J]. Computational Materials Science, 2013, 79:485-494.

[3] Kong C, Sun Z, Gao X, et al. Unit cell of 2.5 dimension C/SiC and its stiffness prediction[J]. Journal of Aerospace Power, 2011, 26: 2459-2467. (In Chinese)

[4] ZHANG B, TANG Z, ZHAO L. Refined generalized method of cells with complex micro-structure of unidirectional composites[J]. Engineering Mechanics, 2012, 29(11): 46-52. (In Chinese)

[5] Dai Q. Prediction of dynamic modulus and phase angle of stone-based composites using a micromechanical finite-element approach[J]. Journal of materials in civil engineering, 2009, 22(6): 618-627.

[6] Xia Z, Zhang Y, Ellyin F. A unified periodical boundary conditions for representative volume elements of composites and applications[J]. International Journal of Solids and Structures, 2003, 40(8): 1907-1921.

[7] Yen C F. Ballistic impact modeling of composite materials[C]//Proceedings of the 7th international LS-DYNA users conference. 2002, 6: 15-23.

[8] Johnson G R, Cook W H. A constitutive model and data for metals subjected to large strains, high strain rates and high temperatures[C]//Proceedings of the 7th International Symposium on Ballistics. 1983, 21: 541-547. Johnson-Cook model

[9] Kulkarni M. Finite element analysis of 2-D representative volume element[J]. 2012.

[10] Zhang C, Xu X, Yan X. General periodic boundary conditions and their application to micromechanical finite element analysis of textile composites[J]. Hangkong Xuebao/Acta Aeronaut Astronaut Sin, 2013, 34(7): 1636-1645. (In Chinese)

[11] Pindera M J, Herakovich C T. Shear characterization of unidirectional composites with the off-axis tension test[J]. Experimental Mechanics, 1986, 26(1): 103-112.

[12] Pagano N J, Halpin J C. Influence of end constraint in the testing of anisotropic bodies[M]//Mechanics of Composite Materials. Springer Netherlands, 1994: 2-16.

[13] Zheng X. Nonlinear strain rate dependent composite model for explicit finite element analysis[D]. The

University of Akron, 2006.

[14] Goldberg R K, Roberts G D, Gilat A. Implementation of an associative flow rule including hydrostatic stress effects into the high strain rate deformation analysis of polymer matrix composites[J]. Journal of Aerospace Engineering, 2005, 18(1): 18-27.

[15] Garoz D, Gilabert F, Sevenois R, et al. Definition of periodic boundary conditions in explicit dynamic simulations of micro-or meso-scale unit cells with conformal and non-conformal meshes[C]//17th European Conference on Composite Materials (ECCM 17). 2016.